

An Ordered Mesoporous Aluminosilicate with Completely Crystalline Zeolite Wall Structure

Yunming Fang and Haoquan Hu*

State Key Laboratory of Fine Chemistry, Institute of Coal Chemical Engineering, Dalian University of Technology, 129 Street, Dalian 116012, People's Republic of China

Received February 18, 2006; E-mail: hhu@chem.dlut.edu.cn

Ordered mesoporous aluminosilicates have gathered considerable research interest as solid acid catalysts and adsorbents, especially in the bulk molecule involved process. Unfortunately, their amorphous walls and corresponding low hydrothermal stability and low catalytic (ion exchange) ability seriously limit their practical application.^{1,2} On the other hand, zeolites have been widely used as shape-selective catalysts and adsorbents in petroleum and chemical processes.³ However, serious diffusion restriction imposed by the micropore limited their use in large molecule involved reactions.⁴ Hence, syntheses of new materials to combine advantages of both zeolites and ordered mesoporous materials are industrially very interesting for such materials, providing great opportunity to overcome the difficulty in bulk molecular catalytic conversion and separation.

Synthesis of crystallized ordered mesoporous aluminosilicate by a conventional supramolecular chemistry-based route is extremely difficult since the molecular mechanism for how zeolite frameworks are actually assembled is still unclear. Until now, only ordered mesoporous material with zeolitic primary units in the wall was synthesized.⁵ A promising alternative to synthesize ordered mesoporous material, which cannot be obtained through other methods, is the nanocasting route by utilization of ordered mesoporous silica or carbon as the hard template.^{6,7} However, previous attempts to synthesize ZSM-5 by using CMK-3 as hard template^{8,9} or recrystallization of CMK-3-filled SBA-15¹⁰ only obtained an agglomerate of ZSM-5 nanocrystals with disordered mesoporous structure or SBA-15 with zeolitic fragments in the mesopore wall. Here we report that an ordered mesoporous aluminosilicate with completely crystalline zeolite pore wall structure, denoted as OMZ-1, was successfully synthesized by recrystallization of SBA-15 using in situ formed CMK-5 as the hard template. The role of CMK-5 carbon material here not only serves as the hard template to preserve ordered mesoporous structure but also kinetically controls the crystallization process to form large crystals.

For the synthesis of OMZ-1, high-quality Al/SBA-15, with a Si/Al ratio of 20, and consequently Al/SBA-15/CMK-5 nanocomposite were synthesized according to the reported procedure.¹¹ Tetrapropylammonium hydroxide (TPAOH, 25 wt % in methanol solution) was then impregnated into the Al/SBA-15/CMK-5 nanocomposite with a TPAOH/SiO₂ molar ratio of 0.2. After methanol evaporation, the final mixture was transferred into a Teflon cup for recrystallization of the amorphous pore wall of Al/SBA-15 at 443 K for 48 h in an autoclave containing enough water to produce saturated steam. The products were washed with distilled water and dried in air at 383 K overnight. The removal of carbon material as well as the organic template was achieved by a controlling combustion step, that is, first heated in nitrogen from room temperature to 823 K with a heating rate of 1 K/min, and then the nitrogen was switched to air and kept at 823 K for 5 h. As-synthesized OMZ-1 was characterized by PXRD, FT-IR, BET,

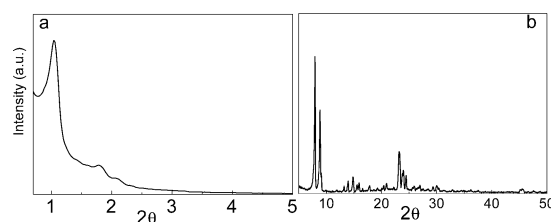


Figure 1. (a) Low- and (b) wide-angle powder X-ray diffraction pattern of OMZ-1.

and TEM. Microporous ZSM-5 with a similar Si/Al ratio was synthesized and characterized for comparison.

In the low-angle PXRD pattern of OMZ-1 (Figure 1a), three well-resolved peaks indexed to the *P6mm* hexagonal symmetry with a lattice constant *a* being 101 Å can be observed. The nitrogen adsorption isotherm shown in Supporting Information also confirms the existence of a uniform mesopore in OMZ-1 with a BJH mesopore diameter of 5 nm. The BJH mesopore surface area and mesopore volume of OMZ-1 are 389.4 m²/g and 0.50 cm³/g, respectively, which are slightly lower than those of parent SBA-15. Considering that the condensation degree of crystallized aluminosilicate is higher than that of amorphous aluminosilicate, the partial loss of surface area and pore volume during recrystallization is reasonable. These results imply that the ordered mesoporous structure of SBA-15 was successfully preserved after recrystallization.

The successful and complete crystallization of SBA-15 was revealed by PXRD and FT-IR patterns. The reflections of OMZ-1 in the wide-angle PXRD pattern (Figure 1b) are very sharp, and the crystal domain size determined from line broadening is larger than 100 nm, which indicated that large domains of SBA-15 are possibly converted to a coherent scattering ZSM-5 phase. The relative intensities of diffraction peaks at similar positions of OMZ-1 are different from those of reference ZSM-5 and the physical mixture of SBA-15 and ZSM-5 (see Supporting Information). Considering that the synthetic conditions (template/SiO₂ ratio, crystallization temperature and time, and template removing method) for both samples are almost the same, such difference is perhaps due to the effect of mesopores in the zeolite crystal structure. The FT-IR patterns of starting SBA-15, the physical mixture of SBA-15 and ZSM-5 in a weight ratio of 1:1, ZSM-5, as well as OMZ-1 are shown in Figure 2. The framework vibration band at 550 cm⁻¹ (double five rings) is the characteristic of MFI-type zeolites¹² and can be used to determine the crystalline degree of these samples. The intensity of the 550 cm⁻¹ band of OMZ-1 is obviously higher than that of the SBA-15/ZSM-5 mixture and comparable with that of reference ZSM-5. The optical density ratio of the 550 cm⁻¹ to the 455 cm⁻¹ bands for OMZ-1 is 0.79, which is very close to that of the reference ZSM-5 sample (0.81),

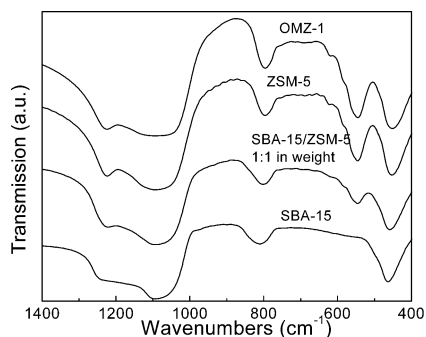


Figure 2. Fourier transform infrared spectra of OMZ-1 and related materials.

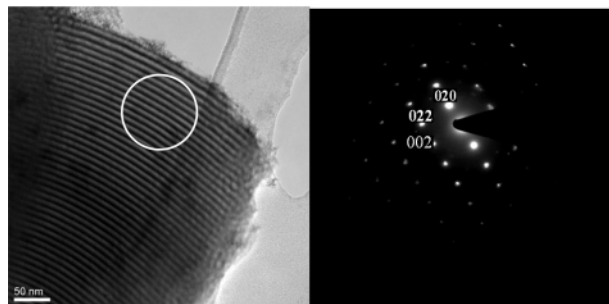


Figure 3. Transmission electron microscopy image and corresponding indexed electron diffraction pattern of OMZ-1; the diameter of the selected area aperture is about 100 nm, as schematically shown in the TEM image.

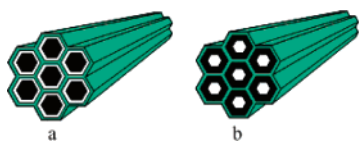


Figure 4. Structural difference between SBA-15/CMK-3 (a) and SBA-15/CMK-5 (b) nanocomposites.

indicating that the mesoporous wall of Al/SBA-15 has been completely crystallized into the MFI structure.

TEM images were recorded with a Philips Tecnai G2 20 operated at 200 kV. Figure 3 is the TEM image viewed parallel to the mesopore channels and the corresponding indexed electron diffraction pattern of OMZ-1. The selected area ED pattern shows the single ZSM-5 crystal (lattice parameters: $a = 19.839$, $b = 20.117$, and $c = 13.386$) nature when viewed down the [100] zone axis. Combination with PXRD and FT-IR analyses suggests that the crystalline ZSM-5 domains extend over areas much larger than the mesopore spacing. The exact nature of the ZSM-5 crystallite size and alignment with respect to the mesopore channel axis is still under investigation. It should be noted that some OMZ-1 with slightly less ordered mesopore structure was also found during the TEM test. There is a slight structural difference between SBA-15/CMK-3¹³ and SBA-15/CMK-5 nanocomposites as shown in Figure 4. Such difference may result in different contact manner between TPAOH and the pore wall of SBA-15 and, consequently, a different ratio between nucleation rate and growth rate of ZSM-5, which controls the crystal size.

The thermal and hydrothermal stability of OMZ-1 was tested by treatment of OMZ-1 both at 850 °C for 4 h in a flow of nitrogen saturated with water vapor at 80 °C and refluxing in boiling water for 120 h. The meso- and microstructure of OMZ-1 was stable after such severe treatment, as confirmed by powder XRD and TEM (see Supporting Information).

The catalytic performance of OMZ-1 in the methylation of 2-methylnaphthalene with methanol was investigated. Detailed Zr

Table 1. Catalytic Results of 2-Methylnaphthalene Methylation^a

catalyst	conv. (%)	β,β -DMN selectivity (%)	2,6-DMN selectivity (%)	2,6/2,7-DMN ratio	2,6-DMN yield (%)
Zr/OMZ-1 (0.5 h)	48	75	46	2.7	18
Zr/ZSM-5 (0.5 h)	10	85	51	2.0	4.6
Zr/OMZ-1 (8 h)	44	78	49	2.6	17
Zr/ZSM-5 (8 h)	6	91	55	2.2	3.1

^a Thermodynamic equilibrium selectivity: β,β -DMN = 36%; 2,6-DMN = 12%.

isomorphic substitution, catalytic reaction, and product analysis methods can be found elsewhere.¹⁴ OMZ-1-based catalyst shows much better catalytic performance than ZSM-5, as shown in Table 1. The higher conversion of 2-MN over Zr/OMZ-1 than over Zr/ZSM-5 may, on first sight, be explained by the difference in the crystal size of OMZ-1 and the reference ZSM-5. However, as previously reported, the conversion of 2-methylnaphthalene over ZSM-5 with a particle size of 70–80 nm, which is smaller than the single ZSM-5 crystallite size in OMZ-1 (proved by XRD and ED pattern), is not higher than 25%;¹⁴ hence it appears reasonable to explain the higher conversion of Zr/OMZ-1 from the improvement in diffusion properties, while selectivity of β,β -DMN and 2,6-DMN, which is much higher than the thermodynamic equilibrium value, is due to the shape-selectivity of the catalyst. The unique catalytic properties further elucidate the claimed structure of OMZ-1.

In summary, our preliminary TEM studies, in combination with PXRD and FT-IR analyses, suggest that an ordered mesoporous aluminosilicate with completely crystalline zeolite wall structure was successfully synthesized, and the crystalline ZSM-5 domains in OMZ-1 extend over areas much larger than the mesopore spacing. The OMZ-1 shows high thermal and hydrothermal stability and catalytic performance in the shape-selective methylation of 2-methylnaphthalene. Further structural characterizations of OMZ-1 as well as synthesis and application of other crystallized ordered mesoporous metallosilicates are still under investigation.

Acknowledgment. Financial support of this work by the Natural Science Foundation of China under Contract Nos. 20276011 and 20376012 is gratefully acknowledged.

Supporting Information Available: Nitrogen adsorption and hydrothermal, thermal test results of OMZ-1, XRD pattern of reference ZSM-5 and SBA-15/ZSM-5 mixture. This material is available free of charge via the Internet at <http://pubs.acs.org>.

References

- (1) Kresge, C. T.; Leonowicz, M. E.; Roth, W. J.; Vartuli, J. C.; Beck, J. S. *Nature* **1992**, *359*, 710–712.
- (2) Corma, A. *Chem. Rev.* **1997**, *97*, 2373–2420.
- (3) Davis, M. E. *Nature* **2002**, *417*, 813–821.
- (4) Christensen, C. H.; Johannsen, K.; Schmidt, I.; Christensen, C. H. *J. Am. Chem. Soc.* **2003**, *125*, 13370–13371.
- (5) Liu, Y.; Zang, W.; Pinnavia, T. *J. Angew. Chem., Int. Ed.* **2001**, *113*, 1295–1298.
- (6) Lu, A. H.; Schmidt, W.; Taguchi, A.; Spliethoff, B.; Tesche, B.; Schüth, F. *Angew. Chem., Int. Ed.* **2002**, *41*, 3489–3492.
- (7) Roggenbuck, J.; Tiemann, M. *J. Am. Chem. Soc.* **2005**, *127*, 1096–1097.
- (8) Yang, Z. X.; Xia, Y. D.; Mokaya, R. *Adv. Mater.* **2004**, *16*, 727–732.
- (9) Sakthivel, A.; Chen, W. H.; Ryoo, R.; Liu, S. B. *Chem. Mater.* **2004**, *16*, 3168.
- (10) Sung, I. C.; Sung, D. C.; Jong, H. K.; Geon, J. K. *Adv. Funct. Mater.* **2004**, *14*, 49–54.
- (11) Sang, H. J.; Seong, J. C.; Ilwhan, O.; Juhyou, K.; Zheng, L.; Osamu, T.; Ryoo, R. *Nature* **2001**, *412*, 169–172.
- (12) Tao, Y. S.; Kanoh, H.; Kaneko, K. *J. Am. Chem. Soc.* **2003**, *125*, 6044–6045.
- (13) Shinae, J.; Sang, H. J.; Ryong, R.; Michal, K.; Mietek, J.; Zheng, L.; Tetsu, O.; Osamu, T. *J. Am. Chem. Soc.* **2000**, *122*, 10712–10713.
- (14) Jin, L. J.; Hu, H. Q.; Wang, X. Y.; Liu, C. *Ind. Eng. Chem. Res.* **2006**, *45*, 3531–3536.

JA061182L